Korean J. Chem. Eng., 35(2), 456-469 (2018)
DOI: 10.1007/s11814-017-0303-y

pISSN: 0256-1115
eISSN: 1975-7220

Biosorptive removal of arsenite and arsenate from aqueous medium using low-cost adsorbent derived from 'Pods of green peas': Exploration of kinetics, thermodynamics and adsorption isotherms

Ashish Kumar*,†, Jayprakash Pandey*, and Satish Kumar**

*Department of Chemistry, Birla Institute of Technology, Mesra, Ranchi 835215, Jharkhand, India
**Department of Chemistry, University Polytechnic, Birla Institute of Technology, Mesra, Ranchi, 835215, Jharkhand, India
(*Received 3 February 2017 • accepted 5 November 2017*)

Abstract−The present work explores the biosorption characteristics of pods of green peas (PGP) for arsenite [As(III)] and arsenate [As(V)] removal from aqueous medium. Optimization of adsorption parameters like contact time, arsenic concentration, temperature, biosorbent dose and pH through batch mode of experiments was studied. Among the different isotherm models, Langmuir for As(III) and Temkin for As(V) provided the best fit for the obtained data of arsenic sorption onto PGP. D-R mean free energy (*E*) indicates the process is physisorption. Thermodynamics studies were found to be endothermic, feasible and spontaneous. Kinetically, adsorption follows the pseudo-second-order kinetics in sorption of As(III) and As(V) both. The desorption studies of exhausted PGP show 81% of As(III) and 72% of As(V) could be leached out. Reusability of biosorbent up to 7th cycles of incessant operation supports their commercial importance with very little effects of common ions on sorption capacity.

Keywords: Biosorption, Pods of Green Peas, Arsenic, Desorption, Isotherm Model, Kinetic

INTRODUCTION

In central-east India, which shares its boundary with the Bengal Delta Plain, the people living in rural and urban areas are directly affected by arsenic-contaminated water [1]. Groundwater of three blocks of Sahebgunj (Sahebgunj, Rajmahal and Udhawa) district in the state of Jharkhand and different area of West-Bengal, India has been found to be alarmingly contaminated with arsenic present above 10 ppb [2,3]. Well-known high arsenic (As) contaminated groundwater areas have been found in Argentina, Chile, Mexico, China, Taiwan, Canada, Hungary, Brazil, Indonesia, India, Pakistan, Bangladesh and Nepal [4-6]. More than 170 million people have been affected by arsenic (As) due to the ingestion of As-contaminated groundwater round the globe [7]. A source of arsenic in natural water depends on the hydrology, local geology and geochemical characteristics of the aquifer materials [8]. Arsenic is an extremely poisonous element because of its toxic effects on human health. In the environment, it is available in the earth's crust and also in the human body [9]. In earth's crust arsenic is twentieth most abundant element, whereas in human beings its rank of abundance is twelfth [10,11]. There are two forms that are common in natural waters: arsenite (AsO_3^{3-}) and arsenate (AsO_4^{3-}), referred to as As(III) and As(V). Pentavalent (+5) or arsenate species are AsO_4^{3-}, $HAsO_4^{2-}$, $H_2AsO_4^-$ while trivalent (+3) arsenite include $As(OH)_3$, $As(OH)_4^-$, $H_2AsO_3^-$ and AsO_3^{3-}. The pentavalent species predominate and are stable in oxygen-rich aerobic environments. Trivalent arsenite predominates in moderately reducing or anaerobic environments such as groundwater. The toxicity of arsenic depends upon its valence state, its organic/inorganic form and the physical aspects leading its adsorption and elimination. In general, trivalent arsenic is more toxic than pentavalent and zero-valent [12]. Arsenic toxicity is very hard to examine because of its ability to convert between oxidation states and organo metalloid forms [13]. Long-term exposure to arsenic-contaminated water increases health risks like skin disease, vascular, conjunctivitis, reproductive, neurological effects, internal cancers and diabetes [14-17].

A number of methodologies are available for the decontamination of arsenic from contaminated water, including co-precipitation or coagulation [18,19], ion-exchange, lime softening, ion exchange [20], reverse osmosis [21]. Most of them are extravagantly costly and have disadvantages such as improper removal, need of high energy and may generate toxic sludge or waste products which are difficult to dispose [22].

At the present time, biosorptive removal of toxic metals and metalloids has also seen significant advancement due to its high sorption efficiency, eco-friendly nature and low cost [23]. Several biosorbents like blue pine and walnut shell [9], stem-powder of *acacia nilotica* [24], pine leaves [25], agricultural residue of 'rice polish' [26], coconut-based agricultural wastes [27] are used as an economical biosorbents for As removal from water. Various other biosorbents have also been reported for efficiently removing As from water. Although various numbers of adsorbents described above have been used for arsenic sorption, the adopted adsorbents are sometimes inadequate for implementation in field-scale. Some of the reasons behind the failure of implementation include extravagant costs, improper handling, lack of regeneration prop-

†To whom correspondence should be addressed.
E-mail: ashishanand8ktr@gmail.com

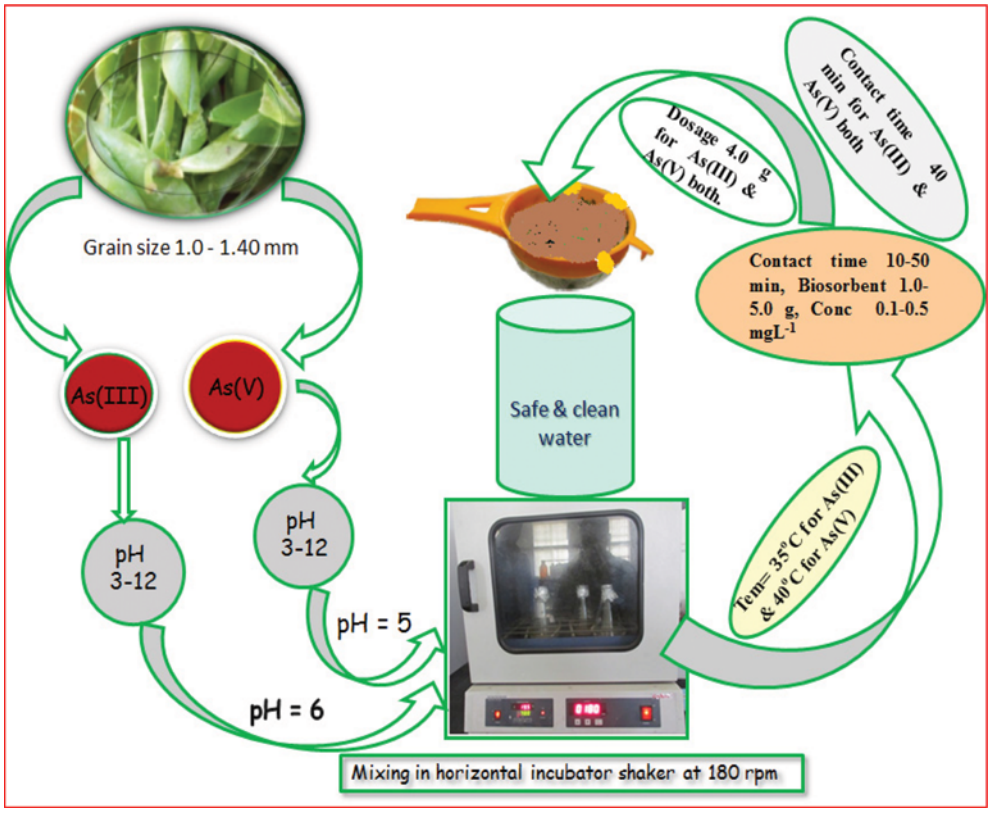

Fig. 1. Schematic representation of sorption studies of arsenite and arsenate from aqueous medium.

erty, leaching of arsenic and not available at local level.

In the present work, an attempt was made to explore the sorption characteristics of splitting the pods of green peas (PGP) for removal of arsenic from aqueous medium and to analyze the data (Fig. 1). The advantages of this biosorbent were not only low-cost and its eco-friendliness, but also its indigenous availability and simplicity of the processes. These will help the villagers to develop their own water purifier. It is also able to procure arsenic free water by self means without any external aids. Green pea is a kind of agriculture waste. It is low-priced and abundantly available lignocellulosic biomass that can serve as potential biosorbent for arsenic removal from aqueous medium. Pea is an annual crop of the winter season, which is a member of the family Leguminosae and grown in different parts of the globe [28]. Pea is cultivated round the globe in approximately six million hectares of cultivable land with an annual production of about 11.7 tones. In India it is cultivated on more than 0.7 million hectares of land, producing about 0.5 million tons annually. It is the second highest important food legume of the world after the common bean [29].

Therefore, in the present work, we focused on characterization and evaluation of arsenic removal efficiency of PGP. The arsenic remediation capacity of PGP was estimated using various physical parameters like biosorbent dose, contact time, arsenic concentration, pH and temperature. In addition to these, kinetics, isotherm model and various thermodynamics parameters were also studied. Further, its commercial applicability regeneration and reuse efficiencies were also evaluated.

MATERIALS AND METHODS

1. Preparation of Biosorbent

PGP was collected from a kitchen as waste residue and washed repeatedly with distilled water to remove dust and soluble impurities, dried in sunlight, then crushed into small fractions and again washed with distilled water. Then again dried in an air oven at 60-70 °C for 30 hours to make PGP crisp. Crisp PGP was crushed into a powder and sieved out in grain size of 1.0-1.4 mm, afterwards washed with double distilled water again to keep free from color and turbidity. Water from the wet biosorbent powder was removed by placing between filter papers and then the biosorbent was placed in an air oven at 60-70 °C for 24 hours to dry completely. It was stored in a plastic container for use as a biosorbent.

2. Preparation of Reagents

All the chemicals used in the experiments were of analytical grade manufactured by Hach, USA, Merck, India, S.D. Fine, Rankem and CDH. Stock solutions of As(III) and As(V) 100 mgL^{-1} each were prepared from sodium arsenite ($NaHAsO_2$) and sodium arsenate ($NaH_2AsO_4{\cdot}7H_2O$), respectively, in Millipore water, and working solutions of the desired concentrations were prepared by diluting the stock solution.

3. Water Sample Collection

Arsenic contaminated groundwater sample was collected from Pathalkudwa, Katatoli, Ranchi, Jharkhand, which is used for domestic and drinking purposes. The contaminated sample was stored in high density polyethylene bottles pre-cleaned with nitric and

hydrochloric acid and thoroughly washed with double distilled water. The pH of the contaminated water was 6.5 at the time of sample collection. Analysis of metal ions in the contaminated water sample was made through ICP-OES. Total dissolved solid (TDS) was estimated through evaporating 100 ml of water sample in China dish. Other physical or chemical parameters were determined by titration methods.

4. Instrumentation and Characterization

The functional groups present in the biosorbent were identified using a Fourier transform infrared (FTIR) spectroscopy (Make and model: Shimadzu, Japan; IR Prestige21). Spectra of the biosorbent before and after arsenic sorption were recorded. The surface morphology of the biosorbent was examined by scanning electron microscope (SEM) (Make and Model: Jeol, Japan; JSM-6390LV) before and after treatment with As(III) and As(V). The distribution of elements on the biosorbent surface was also analyzed before and after treatment with arsenic using energy dispersive X-ray spectrometer (EDS). The As concentration in the water sample was examined using inductively coupled plasma optical emission spectrometer (Perkin Elmer, USA; Optical 2100DV ICP-OES). The pH value was examined by using Orion 720 A^+ ion analyzer equipped with combined fluoride ion selective electrode (Orion 9609 BN Fluoride Combined Electrode) and other physiochemical parameters of water were also analyzed by standard methods [30].

5. Batch Experiments

Biosorbent prepared from PGP was studied to examine its potential for arsenic removal from the contaminated water at the different concentrations range (0.1-0.5 mgL^{-1}). The experiments were done through the batch procedure, where 100 ml of arsenic solution of desired concentration was taken in a conical flask in which optimum amount of PGP was added. The conical flask was shaken for 40 minutes in case of both As(III) and As(V) using a horizontal rotary shaker (shaking speed 180 rpm), until equilibrium was established. Initial concentration was maintained at 0.1 mgL^{-1} for both As(III) and As(V) for every experiment except at the time As concentration was optimized. Further, the biomass of PGP was removed using Whatman filter paper. The residual arsenic concentration was preliminarily analyzed by semi - quantitative arsenic test kit (Quantofix Arsen 10, Germany) and finally using ICP-OES. All experiments were at 35±3 °C for As(III) and 40±2 °C in the case of As(V) except at time of temperature optimization. The pH of the solution was adjusted using either NaOH/HCl solution. All the experiments were conducted twice and the mean values were used in the calculation.

The percent removal of As (R%) and the amount of adsorbate adsorbed per unit weight of biosorbent (mg g^{-1}) at equilibrium (q_e) were calculated using following equations [31].

$$R\% = \frac{(C_o - C_e)}{C_o} 100 \quad (1)$$

$$q_e = \frac{C_o - C_e}{m} V \quad (2)$$

where C_o and C_e (mgL^{-1}) are the As concentrations in solution before adsorption and at equilibrium, respectively, and V is volume of solution (L) and m is the mass (g) of biosorbent used [32-35].

RESULTS AND DISCUSSION

1. SEM and EDS Analysis

Under the optimized conditions of As(III) and As(V) bioreme-

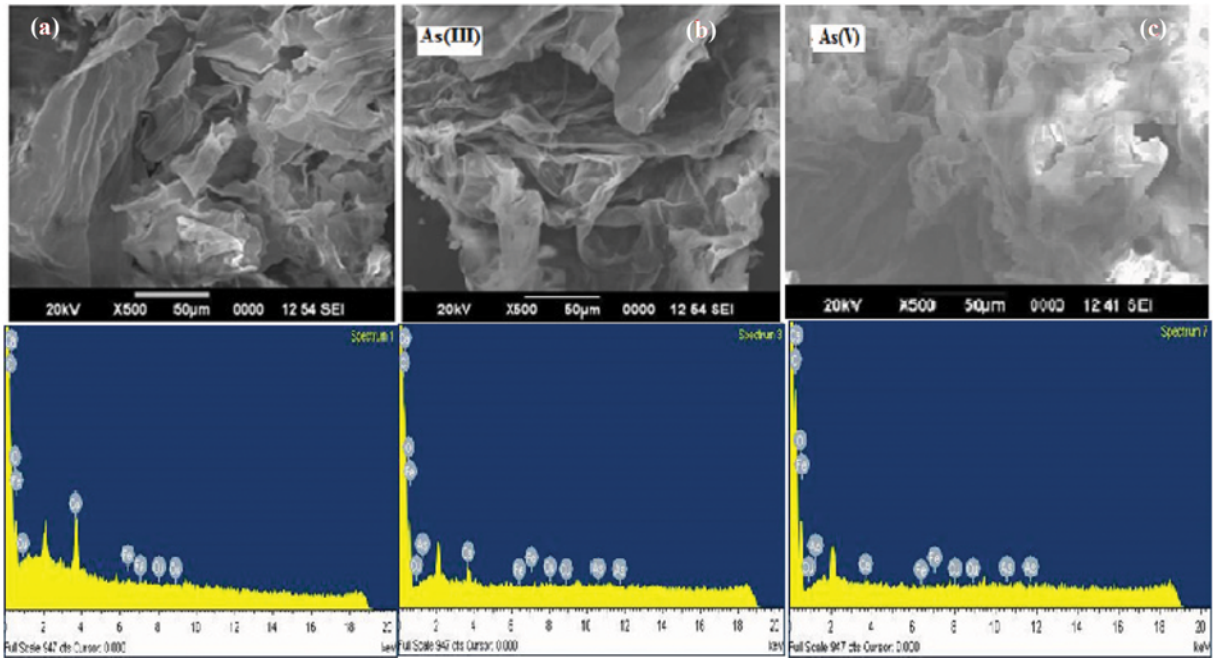

Fig. 2. Scanning electron micrograph and energy dispersive spectra of (a) PGP without use (b) used with As(III) (c) and used with As(V) showing elemental distribution of elements.

diation, the treated biosorbent (PGP) was filtered and dried at 80 °C in oven for 12 hours. Another untreated sample of biosorbent was also placed under the same condition. Then both treated and untreated biosorbent were subjected to SEM and EDS to investigate the change in the surface morphology and elemental distributions of biosorbent before and after treatment. The micrograph taken before the treatment is illustrated in Fig. 2. EDS spectra after sorption studies show the presence of C, Ca, O, Zn and Pt, with an extra peak of arsenic observed other than the prime elements after sorption studies; however, the presence of a peak of Pt was due to coating over the biosorbent during analysis. Again FTIR spectra can give us bond information with functional groups.

2. FTIR Analysis of Biosorbent

FTIR spectra analysis was performed (wave number 4,000-500 cm^{-1}) to determine the functional groups present in biosorbent (PGP). The FTIR spectra of PGP before and after treatment with As(III) and As(V) are shown in Fig. 3. The analysis of the spectra of biosorbent surfaces showed a broad peak at ~3,271 cm^{-1} which may be due to the stretching vibration of O-H of carboxylic acid. The shoulder peak at 2,897 cm^{-1} shows the presence of C-H stretch of alkane.The peak at 2,121 cm^{-1} C≡C can be assigned to stretching of alkynes. The peak at ~1,735 cm^{-1} exemplifies the carbonyl (>C=O) stretch from unionized carboxylic acid. The absorption peak at ~1,635 cm^{-1} shows the stretching vibration of >C=O group. The peak at 1,527 cm^{-1} shows the presence of secondary amine, whereas a peak at 1,323 and 1,060 cm^{-1} indicates the presence of C-N str. of aromatic and aliphatic amine, respectively. After biosorption study with the As(III) and As(V) on PGP, the absorbance peak at 3,271 cm^{-1} of $(OH)_{str}$ shifted to 3,278 and 3,275 cm^{-1} approximately showing strong interaction with As(III) and As(V) substrates. The peak 2,897 cm^{-1} shows interaction with As(III), but does not interact with As(V). The absorbance peak of ~2,121 cm^{-1} (C≡C) shows no interaction with arsenic substrate, which might be due to the absence of coordinating sites. The peak at 1,735.08 cm^{-1} (>C=O) in untreated PGP was shifted to 1,732 cm^{-1} and 1,728 cm^{-1} after absorption with sodium arsenite and

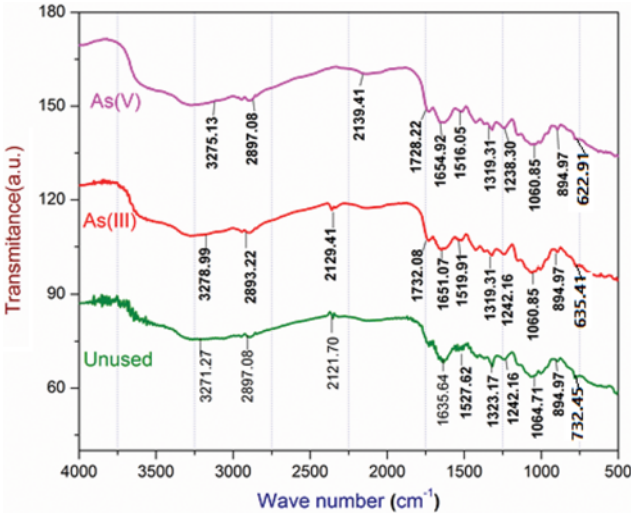

Fig. 3. FTIR spectra of unused (red line) and used with As(III) and As(V) on PGP.

Table 1. Percentage composition of various elements present in PGP

Sorbent	Carbon (wt%)	Hydrogen (wt%)	Nitrogen (wt%)	Sulfur (wt%)	Oxygen (wt%)
PGP	42.750	6.080	0.612	0.416	50.346

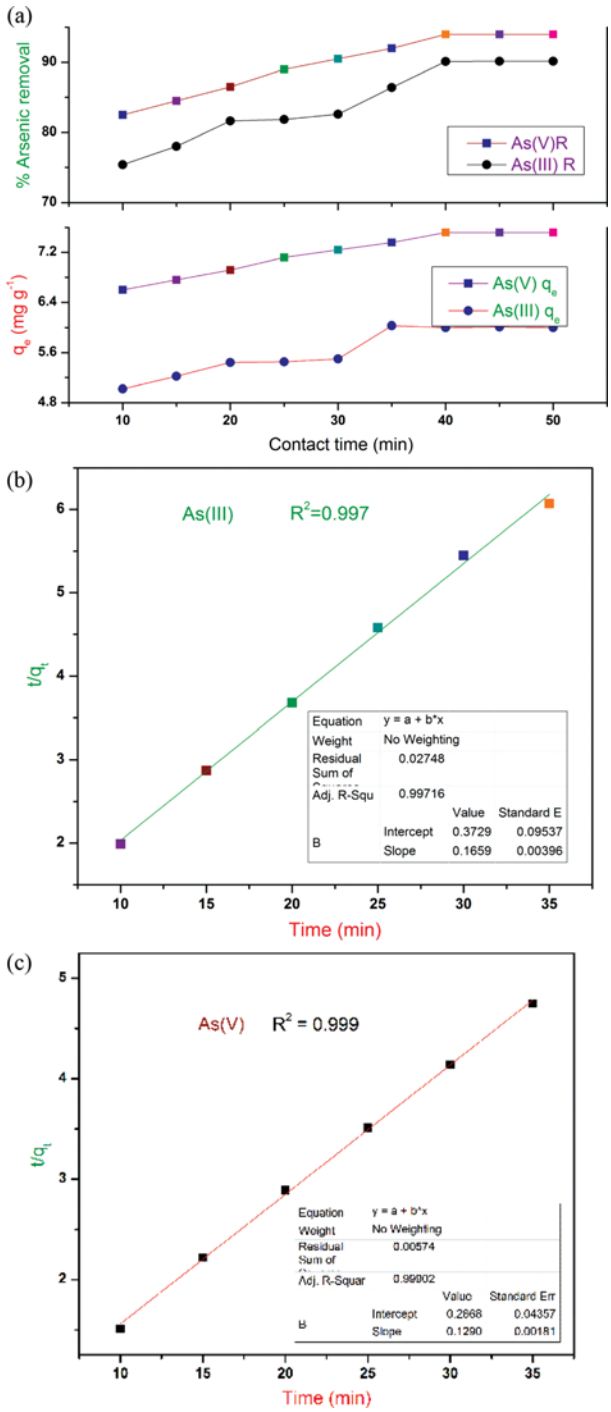

Fig. 4. Effect of contact time on the percent removal and biosorption capacity (q_e) (a) Linear plot of pseudo-second-order kinetics (b) and (c) for As(III) [pH 6.0, biosorbent 40 gL^{-1}, initial concentration 0.1 mgL^{-1} and temperature 35 °C]; and As(V) [pH 5.0, biosorbent 40 gL^{-1}, initial concentration 0.1 mgL^{-1} and temperature 40 °C].

sodium arsenate, respectively. Furthermore, as shown in Fig. 3, the IR spectrum measured before (1,319 and 1,041 cm^{-1}) shows aromatic and aliphatic C-N stretching of the primary amine group and after arsenite and arsenate absorption on PGP of the group, it shifted to a broad spectrum of 1,323 in both arsenite and arsenate, whereas, in case of aliphatic C-N stretching shifted to 1,064 and 1,060 cm^{-1}; these indicate that such functional groups interact with As(III) and As(V) ion in liquid phase. The adsorption peak in 732.45-622.91 cm^{-1} represents C-S stretching of thiol [36].

Furthermore, percentage composition of elements was found by using elemental analysis reported in Table 1 showing low sulfur and nitrogen content. It is conceivable that the existence of NH_2, >NH, -OH, -SH and -COOH groups on the surface of PGP is responsible for the biosorption of As(III) and As(V) from aqueous medium.

3. Effect of Contact Time

Biosorption of As(III) and As(V) with respect to agitation time was investigated at optimized conditions of temperature, concentration of arsenic, pH and biosorbent dose. Fig. 4(a) reveals the increase in percent arsenic removal efficiency of PGP with the contact time. Maximum percent removal efficiencies were achieved 90% for As(III) and 92% for As(V) at the same time span of 40 min. Further, any increase in contact time did not show any considerable changes in percent removal of As(III) and As(V). Therefore, further studies were conducted at 40 min for both As(III) and As(V).

A similar trend was observed in biosorption capacity (q_e) of PGP. Initially, several numbers of biosorption sites were accessible on the biosorbent surface and solute (arsenic) concentration gradient was also high. As(III) and As(V) ions were instantly bonded with biosorption sites on the outer surface of PGP. Therefore, high rate of absorption was observed initially; however, adsorbate ions have to enter to the inner site of adsorbent for adsorption that leads to lower adsorption rate. Once saturation was attained, the arsenic removal capacity remained almost constant.

3-1. Adsorption Kinetics

To examine the contact time of the adsorbate with adsorbent and estimating the reaction coefficients, the kinetic study becomes important in batch mode of experiments. It also helps to examine the biosorption mechanism of arsenic with the PGP. The kinetics of adsorption was computed with the help of three models: pseudo-first-order [37], developed for irreversible adsorption of the solid/liquid system; pseudo-second-order [38], based on equilibrium adsorption capacity; and intra-particle-diffusion model for the comparison of the best fit adsorption mechanism.

Pseudo-first-order kinetics

The mathematical representation of the linear form:

$$\frac{dq_t}{dt} = K_1(q_e - q_t) \tag{3}$$

Integrating Eq. (3), when boundary values t=0 to t=t and q_t=0 to q_t=q_t boundary value gives straight line equation shown as:

$$\log(q_e - q_t) = \log q_e - \left(\frac{K_1}{2.303}\right)t \tag{4}$$

where q_t and q_e indicate the amount of solute adsorbed (mg g^{-1}) at time t and at equilibrium, respectively. K_1 (min^{-1}) is pseudo-first-order rate constant. Linear plot of ln (q_e-q_t) *vs* t gives a straight line; q_e and K_1 were calculated from the intercept and slope of the plot, respectively. Values of various constant of the kinetics are reported in Table 2.

Table 2. Kinetic parameters for the adsorption of arsenic onto PGP at optimized conditions of physical parameters like metal ion concentration, temperature, contact time, adsorbent dose and solution pH

Kinetics	Parameters	Unit	Values	
			As(III)	As(V)
	$q_{e,exp}$	mg g^{-1}	8.21	7.34
	K_f	min^{-1}	0.023	0.069
Pseudo-first-order	$q_{e,cal}$	mg g^{-1}	1.182	2.110
	R^2		0.864	0.961
Pseudo-second-order	K_s	mg $g^{-1}min^{-1}$	0.069	0.062
	$q_{e,cal}$	mg g^{-1}	6.25	7.752
	R^2		0.997	0.999
Intra-particle	K_i	mg $g^{-1}min^{-1/2}$	0.303	0.283
diffusion model	I	mg g^{-1}	4.030	5.681
	R^2		0.803	0.994

Pseudo-second-order kinetics.

The pseudo-second-order kinetics is expressed as:

$$\frac{dq_t}{dt} = K_s(q_e - q_t)^2 \tag{5}$$

Rearranging and integrating Eq. (5) both sides at boundary values t=0 to t=t and q_t=0 to q_t=q_t we get the straight line equation:

$$\frac{t}{q_t} = \frac{1}{K_s(q_e)^2} + \left(\frac{1}{q_e}\right)t \tag{6}$$

where K_s (g $mg^{-1}min^{-1}$) is a pseudo-second-order rate constant, q_t and q_e (mg g^{-1}) are the amount of adsorbate adsorbed at time t and at equilibrium, respectively. Plotting t/q_t *vs* t [Fig. 4(b), 3(c)] gives a straight line, from where K_s and q_e both are estimated from the intercept and slope, respectively. Various constant values of this kinetics are presented in Table 2. The best suitability of the pseudo-second-order kinetics for As(III) and As(V) adsorption onto the biomaterial confirms that the present adsorption process is controlled by both physical and chemical processes over the whole range of adsorbate concentrations studied [39].

3-2. Intra-particle Diffusion Model

For the duration of the batch mode of the experiment, there was a probability of transfer of adsorbate molecules into the pores of adsorbent, which may be the rate controlling step [40]. The intra-particle diffusion model is presented as:

$$q_t = K_i\sqrt{t} + I \tag{7}$$

where I is the intercept and K_i (mg $g^{-1}min^{-1/2}$) is the intra-particle diffusion rate constant which were calculated from the intercept and slope of plot q_t *vs* $t^{1/2}$, respectively. The magnitude of the intercept (I) provides the information concerning the thickness of boundary layer, which causes resistance against external mass

transfer [41]. The higher value of I provides elevated external resistance. The rate constant, the correlation coefficient and other parameters calculated from the graph of the adsorption kinetics models are presented in Table 2.

From the data analysis by different kinetics, it can be concluded that As(III) and As(V) adsorption onto PGP is accompanied by a pseudo-second-order kinetics. The amount of arsenic adsorbed at equilibrium ($q_{e,exp}$), experimental values 8.21, 7.34 mg g^{-1} was found to be close to ($q_{e,cal}$) calculated values 6.25, 7.75 mg g^{-1} for As(III) and As(V), respectively, with the best correlation coefficient (R^2) 0.997 for As(III) and 0.999 for As(V).

4. Effect of Biosorbent Dose

To find the effect of variation in biosorbent mass on percent removal of As, experiments were performed in the dose range of 10-50 gL^{-1}, contact time 40 min, As concentration 0.1 mgL^{-1} for As(III) and As(V) both, whereas pH 6.0 for As(III) and 5.0 for As(V). The results are illustrated in Fig. 5. It was observed that the arsenic removal efficiency increased steadily when the biosorbent dose increased from 1.0 to 5.0 g. However, equilibrium was achieved at 4.0 g biosorbent dose, which was the same for As(III) and As(V) both, but any significant effect on percent arsenic removal was not observed with the increase in the amount of biosorbent. The percent removal of arsenic elevated with biosorbent dose, which is obvious because the number of adsorption sites and surface area increased. Further, no effect on As removal was perceived beyond 82.5% for As(V) and 54% for As(III), because adsorption equilibrium was achieved between free As and PGP. Hence, an optimized value 4.0 g of PGP could be chosen for further examination.

The lower removal efficiency of As(V) ions in comparison to As(III) ions could be explained as in the aqueous medium arsenate ions (AsO_4^{3-}) are larger than arsenite ions (AsO_3^{3-}), so their approachability towards active sites of adsorption is poor. Hence As(III) species of arsenic was more removed than As(V).

5. Effect of pH

The pH of the aqueous medium is a significant controlling parameter in the biosorption process. The pH of arsenic contaminated water sample was supposed to be changed during the process of biosorption as the solution of arsenic was not buffered. The effect of pH on As removal from aqueous medium was studied under optimized contact time 40 min, As concentration 0.1 mgL^{-1}, biosorbent dose 4.0 g, same in both the state, whereas temperature 35 °C, 40 °C for As(III) and As(V), respectively. It was found that pH had a noticeable effect on As uptake in this exploration; Fig. 6 shows that percent arsenic removal increased with the pH of solution up to 6 for As(III) and 5 for As(V). Again removal efficiencies, reduced with further increase in pH.

In case of arsenite, a sharp increase in percentage sorption was observed in the pH range of 3-6, and optimum removal of 96% was obtained at pH 6; thereafter negative trends were observed. At lower pH, the adsorbent surface specially -NH_2 groups are highly protonated and such situation favored the process of biosorption due to electrostatic attraction between opposite charged species [42]. To increase in pH of the system, the extent of protonation of

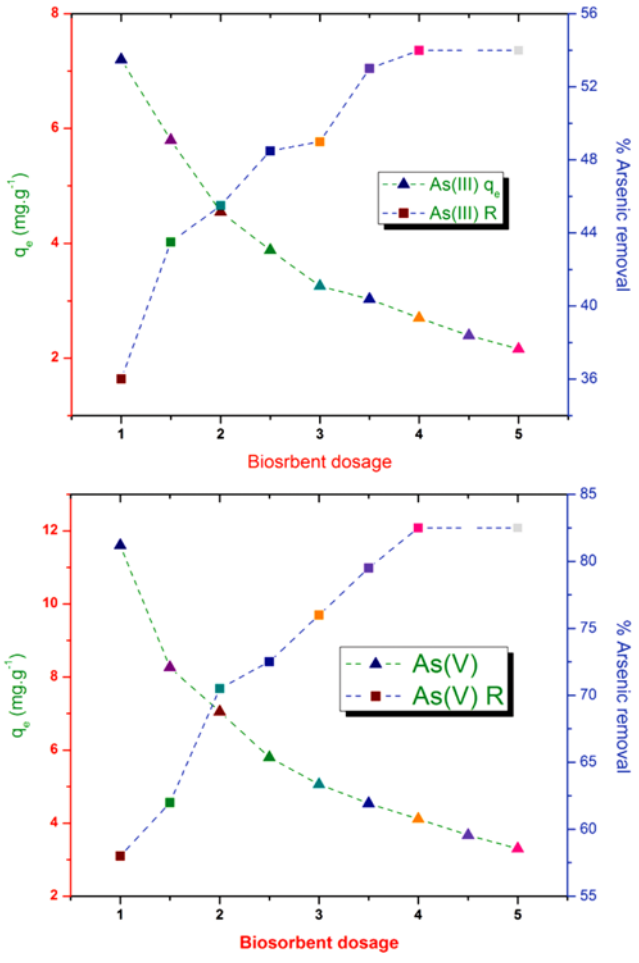

Fig. 5. Effect of biosorbent dosage on the removal of As (III) [pH 6.0, initial concentration 0.1 mgL^{-1}, temperature 35 °C and contact time 40 min]; As(V) [pH 5.0, initial concentration 0.1 mgL^{-1}, contact time 40 min and temperature 40 °C].

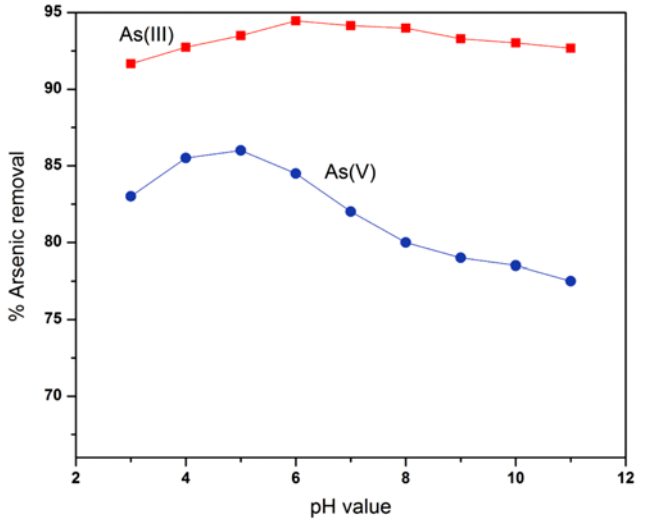

Fig. 6. Effect of pH on the percent removal of As(III) [initial concentration 0.1 mgL^{-1}, biosorbent 40 gL^{-1} temperature 35 °C, contact time 40 min]; As(V) [initial concentration 0.1 mgL^{-1}, biosorbent 40 gL^{-1}, contact time 40 min and temperature 40 °C].

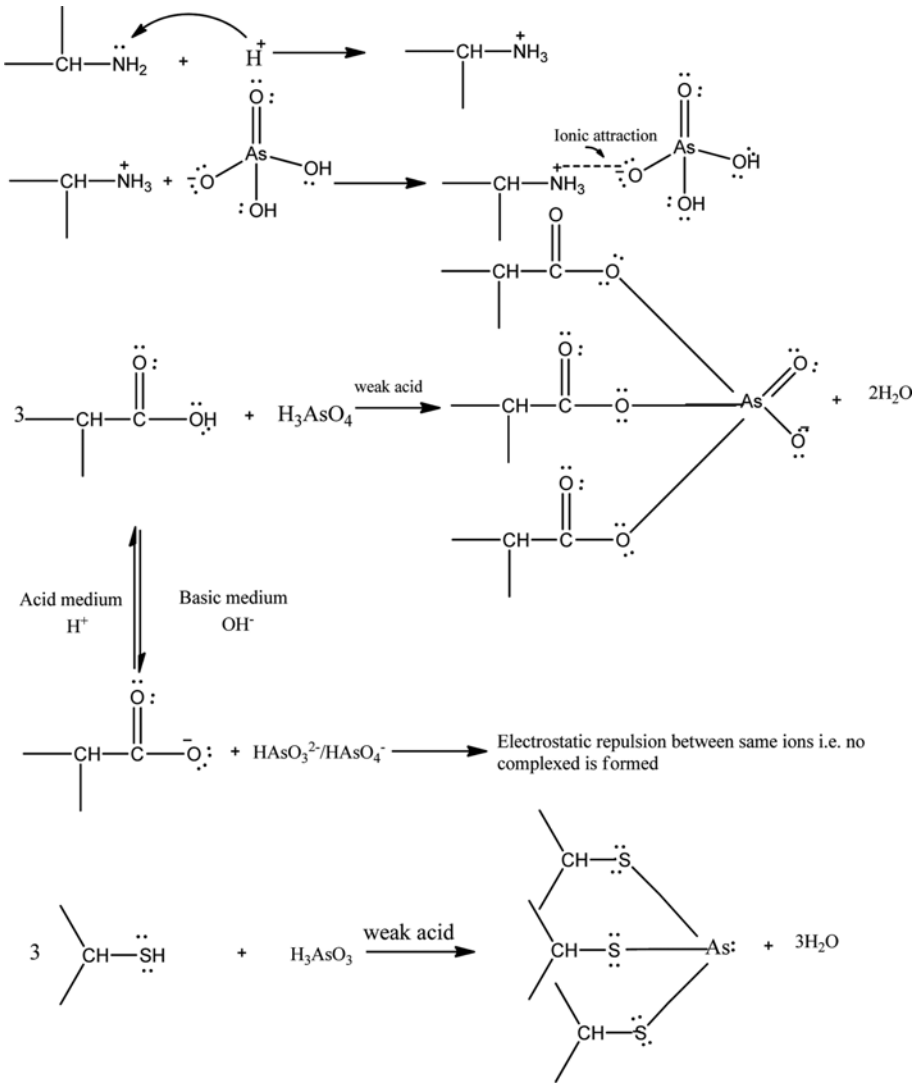

Scheme 1. Systematic representation of interaction of As(III) and As(V) with active functional groups.

biosorbent surface (-NH_2 group) reduces regularly because of decrease of sorption efficiency. At higher pH (>6) of the medium, neutral or anionic species of arsenite, i.e., $H_2AsO_3^-$ and $HAsO_3^{2-}$ predominates. IR analysis of the PGP referred to the presence of functional groups like -COOH, -NH_2, -OH and -SH on the biosorbent surface. These functional groups are considered as active sites for sorption of arsenite and arsenate.

In case of arsenate, the percentage removal increased from 82.5% to 86% with an increase in pH from 3 to 5, and then it decreased with further increase in pH (up to 11). It is well-known that arsenate is more strongly adsorbed than arsenite at the pH either acidic or neutral [43]. In extremely acidic conditions, less adsorption occurs due to a neutral state of H_3AsO_4 which does not interact with positive centers. Whereas, at pH 4-7, As(V) predominates as $H_2AsO_4^-$, $HAsO_4^{2-}$ and AsO_4^{3-} ionic state [7], but at alkaline pH active center of biosorbent is not protonated and becomes either neutral or negative center by releasing H^+ from proton donating group (-COO^-, -NH^-, -O^-) [9]. A repulsive force may develop between the same charges, which decreases the arsenate sorption at higher pH. The possible mechanism for the interaction of above mentioned functional groups with arsenite and arsenate is represented in Scheme 1

According to the bibliographic information, agricultural byproducts usually are composed of lignin and cellulose as major constituents and may also include other polar functional groups of lignin, which includes alcohols, aldehydes, ketones, carboxylic, phenolic, thiol and ether groups. The presence of such active functional groups is again confirmed by FTIR spectrum analysis in the present work. The possible mechanism for the interaction of above mentioned functional groups with As(III) and As(V) is proposed as Scheme 1.

6. Effect of Solution Concentration

The percent removal efficiency as well as the absorption capacity (q_e) of PGP was studied by varying the arsenic concentration in the range of 0.1-0.5 mgL^{-1}. Such steps were performed under optimized conditions of biosorbent dose 4.0 g and contact time 40 min. It was observed that arsenic removal efficiencies decreased as initial concentration of arsenic was increased. The results are illus-

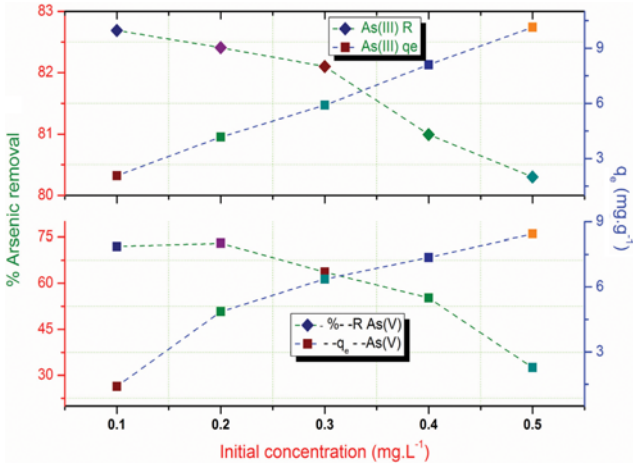

Fig. 7. Effect of initial metal ion concentration on the percent removal and absorption capacity (q_e) of As(III) [pH 6.0, biosorbent 40 gL^{-1}, temperature 35 °C and contact time 40 min]; As(V) [pH 5.0, biosorbent 40 gL^{-1}, contact time 40 min and temperature 40 °C].

trated in Fig. 7. Actually, with an increase in the concentration of arsenic in aqueous medium, the available coordination sites of adsorbent remained constant; therefore, saturation was achieved and that shows the decreasing trend of biosorption efficiency. However, maximum removal efficiency 82.6% for As(III) and 64% for As(V) was attributed to lower concentrations 0.1 mgL^{-1}, which is the same for As(III) and As(V) both. Hence, for further studies arsenic concentration of 0.1 mgL^{-1} was adopted as an optimum value.

The principle of adsorption isotherms is to establish the relationship between the adsorbate absorbed per unit mass of adsorbent (q_e) and equilibrium solute concentration (C_e). To evaluate the adsorption efficiencies of this process, experimental data were modeled after Langmuir, Freundlich, Temkin and Dubinin-Radushkevich (D-R) isotherms in the present exploration. The isotherm studies were conducted by varying the concentration of As(III) and As(V) from 0.1 to 0.5 mgL^{-1} at the optimized conditions of temperature, contact time, pH and biosorbent dose.

6-1. Adsorption Isotherm Studies

A valuable characteristic of modern engineering is the potential to adequately model the behavior before going to large-scale investment. For developing a good model some basic knowledge is required as fundamental theoretical understanding, observation of experiments and measurements of the system. Thus, adsorption equilibrium relationship at a given temperature is called the adsorption isotherm. The adsorption isotherm parameters concerning the Langmuir, Freundlich, Temkin and D-R isotherm models were applied to the experimental data, collected from batch experiments at 35 °C for As (III) and 40 °C for As(V).

6-2. Langmuir Isotherm

The main assumption of Langmuir isotherm is the monolayer formation of the solute on the surface of adsorbent without interaction between the solute molecules [44]. The straight line equation of Langmuir adsorption isotherm is represented as:

$$\frac{1}{q_e} = \frac{1}{K_L q_m C_e} + \frac{1}{q_m} \tag{8}$$

where K_L (L mg^{-1}) and q_m (mg g^{-1}) are Langmuir constants concerned with adsorption energy and maximum adsorption capacity [41], respectively. The magnitude of K_L and q_m was calculated from the intercept and slope of plot $1/q_e$ *vs* $1/C_e$, respectively. The various constants and the correlation coefficient values are presented in Table 3.

To predict whether the adsorption process is favorable or unfavorable for the Langmuir type adsorption isotherm, the separating factor (R_L) was calculated using the given equation:

$$R_L = \frac{1}{1 + K_L C_o} \tag{9}$$

where K_L is the Langmuir isotherm constant and C_o is the ini-

Table 3. Various constant values of Langmuir, Freundlich, Temkin and D-R adsorption isotherm for the adsorption of arsenic onto PGP at optimized conditions of physical parameters like metal ion concentration, temperature, contact time, adsorbent dose and solution pH

Isotherm models	Parameters	Unit	Values	
			As (III)	As(V)
Langmuir isotherm model	K_L	L mg^{-1}	3.05	16.18
	R_L	(separation factor)	0.766-0.180	0.38-0.109
	q_m	mg g^{-1}	43.48	10.42
	R^2		0.997	0.926
Freundlich isotherm model	K_F	mg$^{1-(1/n)}$L$^{1/n}$g^{-1}	0.174	0.501
	n		1.220	4.424
	R^2		0.989	0.933
Temkin isotherm model	A	L mg^{-1}	0.082	0.085
	B_1	J mol^{-1}	4.510	2.650
	R^2		0.951	0.952
D-R isotherm model	X_m	mg g^{-1}	8.004	8.174
	R^2		0.835	0.592
	E	kJmol^{-1}	0.259	0.447

tial concentration of adsorbate. The process of Langmuir isotherm is favorable if the magnitude lies in the range $0<R_L<1$, if $R_L=1$, it is linear; if $R_L=0$, it is irreversible; and if $R_L>1$, the isotherm process is unfavorable [45,46]. The value of R_L was estimated for the entire concentrations range and was found between 0 and 1, confirming favorable adsorption condition.

6-3. Freundlich Isotherm

The Freundlich isotherm is most commonly used to explain adsorption on a surface having heterogeneous energy distribution. The straight line equation of Freundlich isotherm can be expressed as [47]:

$$\log q_e = \log K_F + \left(\frac{1}{n}\right)\log C_e \quad (10)$$

where n and K_F are constants representing adsorption intensity and adsorption capacity, respectively, related to the nature of adsorbate and absorbent. The values of n and K_F were found from the slope and intercept of the plot log q_e *vs* log C_e, respectively, and the respective constant values are given in Table 3. The magnitude of n is much higher than unity for both As(III) and As(V), hence indicating that biosorption process by PGP is favorable. However, comparing the correlation coefficient values of Langmuir with Freundlich isotherms, the Freundlich isotherm model was found more applicable in the case of As(III) than that of As(V).

6-4. Temkin Adsorption Isotherm

The Temkin isotherm model is based upon the interaction between adsorbate/adsorbent in solution phase. The main assumption of this model is that the heat of adsorption of whole molecules in the layer decreases in a linear way with coverage due to adsorbate-adsorbate repulsion between same ions [48]. The linear form of this isotherm can be represented as follows:

$$q_e = B_1 \ln A + B_1 \ln C_e \quad (11)$$

where A (L mg^{-1}) is an equilibrium binding constant, refers to maximum binding energy and B_1 (J mg^{-1}) is related to the heat of adsorption [49]. The constant B_1 and A values are found from the slope and intercept of the plot q_e *vs* ln C_e, respectively, and their values are reported in Table 3. The correlation coefficient (R^2) values of Temkin isotherm are 0.951 and 0.926 for As(III) and As(V), respectively, indicate that this model is more approving for As(III) than that of As(V).

6-5. Dubinin-Radushkevich (D-R) Isotherm

The Langmuir and Freundlich isotherms are not able to explain the adsorption mechanism. To evaluate the nature of adsorption, the data were also applied to D-R isotherm [50], which can be expressed as:

$$\ln q_e = \ln X_m - \beta\varepsilon^2 \quad (12)$$

$$\varepsilon = RT\ln\left(1+\frac{1}{C_e}\right) \quad (13)$$

where C_e (mgL^{-1}) is equilibrium concentration and q_e (mg g^{-1}) is the amount of arsenic adsorbed by per unit weight of PGP, β and X_m are constants related to adsorption energy and theoretical saturation capacity, respectively. R is the universal gas constant and T is temperature (K). The constants β and X_m were calculated from the slope and intercept of plot ln q_e *vs* ε^2, respectively. The adsorption mean energy (E) was calculated from β - value by using an equation:

$$E = \frac{1}{\sqrt{-2\beta}} \quad (14)$$

The magnitude of E is helpful for estimating the kind of adsorption. If it lies between 8 to 16 $kJmol^{-1}$, the kind of adsorption is ion exchange [51] and if the magnitude of $E<8$ $kJmol^{-1}$, it is physisorption [52]. The various constant values are reported in Table 3.

The experimental data of adsorption studies together with the calculated data from Langmuir, Freundlich, Temkin and D-R isotherm linear regression analysis, curve for As(III) and As(V) is

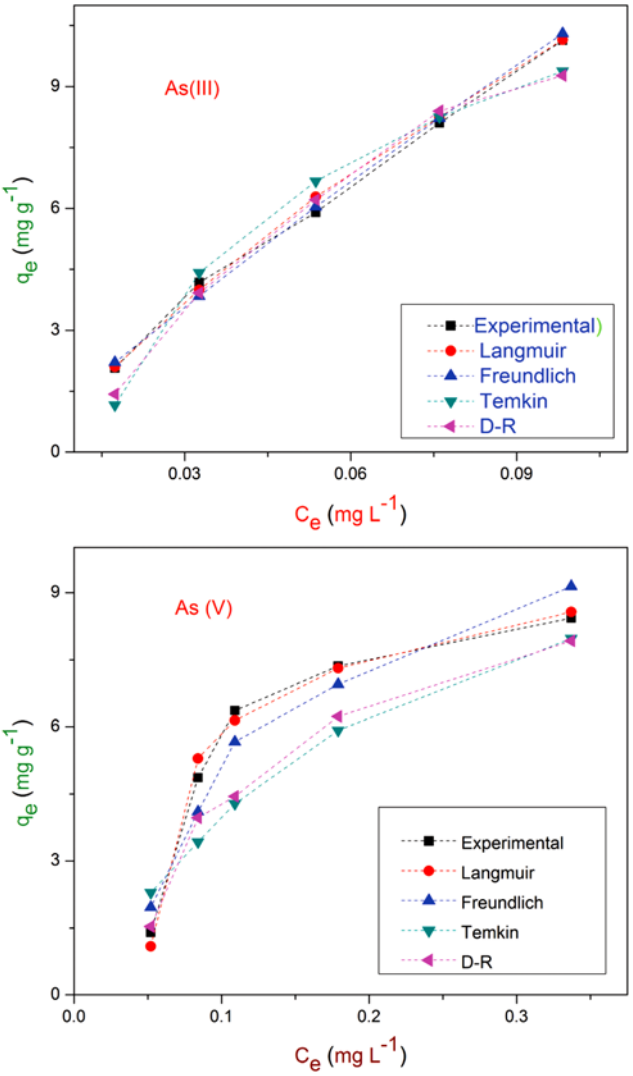

Fig. 8. Adsorption isotherm modeling of As(III) and As(V) removal using PGP using linear regression analysis As(III) [pH 6.0, initial concentration 0.1 mgL^{-1}, temperature 35 °C and contact time 40 min, biosorbent dosage 40 gL^{-1}]; As(V) [pH 5.0, initial concentration 0.1 mgL^{-1}, contact time 40 min temperature 40 °C and biosorbent dosage 40 gL^{-1}].

shown in Fig. 8. On the basis of minimum differences between $q_{e,exp}$ and $q_{e,cal}$, Langmuir for As(III) and Temkin for As(V) are proved to be the most applicable isotherm model for the adsorption of arsenic species onto PGP.

However, to determine the most correct isotherm model for biosorption of As(III) and As(V) on the PGP, the error function analysis was attempted. It was performed by the use of a linear least square method using Microsoft excel and SPSS 13.0 statistical software. Five different frequently used error functions were applied to evaluate the error deviation between the experimental and calculated equilibrium data using linear analysis. The mathematical equations of different error functions applied in this study are given below:

(a) The average relative errors, deviation (ARED) [53].

$$ARED = \frac{1}{N}\Sigma_{k=0}^{n}\left|\frac{q_{e,cal}-q_{e,exp}}{q_{e,exp}}\right|100 \quad (15)$$

where N is number of experimental data point, $q_{e,cal}$ and $q_{e,exp}$ (mg g^{-1}) are calculated and experimental adsorption capacity, respectively.

(b) The sum of square of the errors (SSE):

$$SSE = \Sigma(q_{e,cal}-q_{e,exp})^2 \quad (16)$$

(c) Marquardt's percent standard deviation (MPSD):

$$MPSD = 100\sqrt{\frac{1}{N-P}\Sigma_{i=1}^{n}\left(\frac{q_{e,exp}-q_{e,cal}}{q_{e,cal}}\right)_i^2} \quad (17)$$

(d) The hybrid fractional error function (HYBRID)

$$HYBRID = \frac{1}{N-P}\Sigma\left|\frac{q_{e,exp}-q_{e,cal}}{q_{e,exp}}\right|100 \quad (18)$$

The sum of absolute errors (SAE):

$$SAE = \Sigma_{i=1}^{n}|q_{e,cal}-q_{e,exp}| \quad (19)$$

The values of all above-mentioned error functions are reported in Table 4. After analysis of the data, it appears that the Langmuir model for As(III) and Temkin model for As(V) are the most suitable to adequately elucidate the studied adsorption phenomenon. Indeed, the maximum R^2 value and minimum ARED, SSE, SAE, MPSD and HYBRID value were observed for As(III) and As(V). Such trends are performed in the same way as that observed by other researchers [41,54].

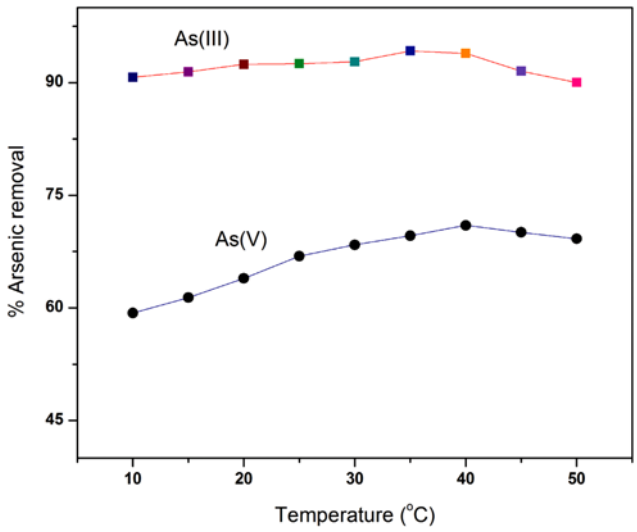

Fig. 9. Effect of temperature on the removal of As(III) [pH 6.0, initial concentration 0.1 mgL^{-1}, biosorbent dosage 40 gL^{-1} and contact time 40 min]; As(V) [pH 5.0, initial concentration 0.1 mgL^{-1}, contact time 40 min and biosorbent dosage 40 gL^{-1}].

7. Effect of Temperature

The percent removal efficiency of As(III) and As(V) was studied in the temperature range 10-50 °C, under optimized conditions of experimental setup. The results are shown in Fig. 9. The curves are sharp, continuous and leading towards equilibrium when maximum removal occurs [92% at 35 °C and 68% at 40 °C for As(V)]. Further increase in temperature resulted in lower As removal efficiency. Actually, with increase in temperature causes enhancement in the surface activity and kinetic energy of dissolved metal ions which fastens the biosorption process. At higher temperatures, physical structure of biosorbent surface changes, which may decrease the biosorption efficiency of PGP. In the present investigation, the optimum value of temperature was selected as 35 °C for As(III) and 40 °C for As(V). Experiments were performed in a horizontal incubator shaker, and lower temperature was maintained by placing a conical flask containing the test sample in an ice bath.

Table 4. Adsorption isotherm error data concerned with the biosorption of arsenic onto PGP using six commonly used functions showing the applicability of Langmuir for As(III) and Temkin for As(V)

Error functions	R^2	ARED	SSE	SAE	MPSED	HYBRID
As(III)						
Langmuir	**0.997**	**1.5411**	**0.2080**	**0.7600**	**0.3912**	**4.7720**
Freundlich	0.989	4.0659	0.1948	0.9000	0.6731	6.7765
Temkin	0.951	14.4201	5.7775	2.8300	12.6756	24.0335
D-R	0.828	10.9351	1.4202	2.3800	6.4059	18.2252
As(V)						
Langmuir	0.926	7.4499	0.1978	0.8956	18.2104	12.4165
Freundlich	0.933	11.2032	1.4829	2.3889	23.8482	18.6720
Temkin	**0.952**	**6.3302**	**0.6705**	**0.4299**	**0.9471**	**4.8836**
D-R	0.592	21.4339	6.0503	4.5900	36.7927	35.7231

Table 5. Thermodynamic parameters for the adsorption of As(III) and As(V) onto PGP at optimized conditions of physical parameters like metal ion concentration, temperature, contact time, adsorbent dose and solution pH

Equations	Thermodynamic parameters	Plot	Values	
			As(III)	As(V)
		283 K	−0.230	−0.894
	ΔG^o (kJ mol^{-1})	293 K	−0.192	−1.388
$\Delta G^o = -RT \ln K_c$	Temperature range	303 K	−0.188	−1.990
		313 K	−0.162	−2.316
		323 K	−0.265	−2.175
$\ln K_c = \frac{\Delta S^o}{R} - \frac{\Delta H^o}{RT}$	ΔH^o (kJ mol^{-1})	ln K_c *vs* 1/T	0.896	0.141
	ΔS^o (kJ mol^{-1}K^{-1})		2.340	54.040
$\log(1-\theta)$	S^*	$\log(1-\theta)$ *vs* 1/T	0.009	0.012
$= \log S^* + \frac{E_a}{2.303RT}$	E_a (kJ mol^{-1})		10.820	8.424

SORPTION THERMODYNAMICS

Thermodynamic parameters--the change in free energy of adsorption (ΔG^o), enthalpy change (ΔH^o) and entropy change (ΔS^o)--can be estimated by using the following equation in the temperature range 10-50 °C [55]:

$$K_c = \frac{C_{Be}}{C_e} \tag{20}$$

where C_{Be} is concentration of As(III) and As(V) on absorbent and C_e is equilibrium concentration. The K_c value is used in Eqs. (21) and (22) for estimating the values of ΔG^o, ΔH^o and ΔG^o. The van't Hoff equation can be written as:

$$\Delta G^o = -RT \ln K_c \tag{21}$$

where K_c is distribution coefficient, R is gas constant and T is temperature (K). The estimated ΔG^o values for As(III) and As(V) are found to be negative in the entire range of temperature, which reveals the process of absorption as spontaneous.

Further, the relationship between K_c *vs* ΔS^o *vs* ΔH^o as a function of temperature can be written as:

$$\ln K_c = \frac{\Delta S^o}{R} - \frac{\Delta H^o}{RT} \tag{22}$$

The values of ΔS^o and ΔH^o can be calculated from the intercept and slope of the plot of ln K_c *vs* 1/T, respectively. Sticking probability (S^*) is the function of the adsorbate/adsorbent system and often depends on temperature. It is to measure the potential of adsorbate which remained on the surface of adsorbent [54]. The equation is written as:

$$S^* = (1-\theta)e^{-\frac{E_a}{RT}} \tag{23}$$

Rearranging Eq. (23) and taking the log of both sides:

$$\log(1-\theta) = \log S^* + \frac{E_a}{2.303RT} \tag{24}$$

where θ is surface coverage area and E_a is the activation energy

$$\theta = \left(1 - \frac{C_e}{C_o}\right) \tag{25}$$

The values of S^* and E_a were calculated from the intercept and slope of the plot log $(1-\theta)$ *vs* 1/T, respectively. The positive value of ΔH^o and activation energy (E_a) reveals the adsorption process is endothermic. Also, sticking probability (S^*) of PGP surface was found to be 0.0095 for As(III) and 0.0126 for As(V) which is less than zero, which refers to the process as physisorption. All the values of thermodynamic parameters are reported in Table 5.

APPLICATION ON NATURAL ARSENIC CONTAMINATED WATER SAMPLE

For the applicability of biosorbent, real arsenic-contaminated groundwater sample was collected. 100 ml of a test sample of initial pH 6.5 was taken in a stoppered conical flask and then put into horizontal a incubator shaker under aforementioned optimized experimental setup. It was filtered and the residual was analyzed for metal ions using ICP-OES, and the other physiochemical

Table 6. Characteristics of field water samples

Parameters	Before biosorption[a]	After biosorption[a]
pH	7.08	6.08
TDS (mgL^{-1})	635	674
EC (μs/cm)	1319	1254
Salinity	0.69	0.84
Cl^- (mgL^{-1})	33.66	27.1
ORP (mv)	251.6	189.2
NO_3^- (mgL^{-1})	2.72	1.47
Ca (mgL^{-1})	111.5	123.1
Fe (mgL^{-1})	1.574	0.047
Mg (mgL^{-1})	17.86	29.24
Mn (mgL^{-1})	0.994	0.891
As (mgL^{-1})	0.096	BDL[#]

[a]All values are reported in average of five readings with RDS (%) 1.64-2.34

[#]Below detection limit

Table 7. Comparison of the sorption characteristics of As(III) and As(V) from contaminated water by various sorbents

Biosorbents	pH range	Optimum pH value	Maximum sorption capacity (mg g^{-1})	Ref.
Coconut shell	2-12	10	0.368 As(III)	[1]
Pine leaves	1-10	4	3.27 As(V)	[2]
Mango leaf powder	2-12	8	174.93 As(III)	[3]
Lemon residues ($FeCl_3$ treated)	2-10	7	0.474 As(V)	[4]
Magnetic (Fe_3O_4) wheat straw	3-11	7-9	3.8 As(III)	[5]
Rice polish	2-10	4	0.14 As(V)	[6]
Coconut coir pith	2-10	7	13.57	[7]
Orange juice residue	2-14	4	132 As(V)	[8]
Orange juice residue	2-14	10	97 As(III)	[8]
Fe-modified bamboo charcoal	2-9	4-5 As(III) 3-4 As(V)	7.237 As(III) 19.771 As(V)	[9]
Sugarcane bagasse treated with hydrous ferric oxide	2-10	5	24 As(V)	[10]
Potato peel	2-9	5	2.17 μg g^{-1}	[11]
Peel of green peas	3-11	6-7 As(III) 4-5 As(V)	43.48 As(III) 10.42 As(V)	Present work

parameters of water were analyzed by standard methods [32]. The results reported in Table 6 clearly reveal that most of the physiochemical parameters were brought under the permissible limit of WHO guidelines 1996 and arsenic was also below the detection limit.

A comparison of the biosorption capacity (q_m) of As(III) and As(V) with some treated and untreated natural biosorbent (Table 7) reveals that the natural biosorbent PGP has effective biosorption capacity (q_m) of As(III) and As(V) a portable pH range of water and lower As(III) and As(V) concentrations. Also, the cost of the preparation of treated compounds is very high and probability of contamination of water with some foreign elements is also frequent as compared to the prepared biomass PGP. It is economically feasible because the indigenous availability is at large scale. These can be implemented in large scale treatment of contaminated water.

INTERFERING IONS STUDIES

Potable water may contain many ions, which may compete with arsenic for active sites of sorption. The arsenic removal from water in the presence of interfering ions may be affected due to formation of complex or competition for common adsorption sites, the result of which observed is shown in Table 8. For the studies of interfering ions, different cations and anions as mentioned in Table 8 were added in collecting arsenic contaminated water sample in the concentration of ten times higher than the permissible limit. Cations Fe^{3+}, Zn^{2+} and K^{+} enhance the biosorption efficiency due to effective electrostatic interaction between opposite charges. Whereas, Cr^{6+}, Pb^{2+}, Cu^{2+}, Ni^{2+} and Ca^{2+} reduce arsenic absorption capacity. On the other hand, anions such as NO_3^- and Cl^- do not significantly influence arsenic adsorption, whereas F^- and SO_4^{2-} decrease the absorption capacity effectively. It may be explained on the basis of common ion repulsion and ionic sizes. Outcomes are in the same way with that of other investigators [24,46].

Table 8. Inferences of common ions on biosorption of arsenic onto biomass (PGP)

Cations	%Biosorption	Anions	%Biosorption
Arsenic	94±0.03	Cl^-	93±0.02
Pb^{2+}	90.5±0.04	F^-	92±0.03
Cr^{6+}	74±0.02	SO_4^{2-}	91.5±0.04
Cu^{2+}	90±0.03	NO_3^-	93.5±0.02
Ni^{2+}	81.5±0.02		
Fe^{3+}	99.4±0.05		
Ca^{2+}	83.5±0.04		
Zn^{2+}	99.2±0.02		
K^{+}	98.6±0.06		

DESORPTION AND REUSE STUDIES

Desorption and reuse of the biosorbent for subsequent removal of metal ions from aqueous system contributes to the economic importance of the biosorption process. For desorption studies of As(III) and As(V) from loaded PGP through batch mode of the experiment was conducted. A known amount of exhausted PGP (3.0 g) and 100 ml of an eluting agent like HCl and HNO_3 having concentration range 0.01-0.1 M was taken (one by one) in a 250 ml conical flask and was put in a horizontal shaker for 40 min at 30 °C temperature. The PGP was separated from solution using Whatman filter paper. Then the strength of arsenic (mgL^{-1}) was determined from ICP-OES. Fig. 10 shows the desorption action of As(III) and As(V) from used PGP after eluting it with HCl and HNO_3. Usually, the desorption rate of As increases with the increase in strength of the eluting agent. From the Fig. 10, maximum desorption occurs at 48% for As(III) and 72% for As(V) using nitric acid (0.1 M). However, it was found 40.7% for As(III) and 81% for As(V) using hydrochloric acid (0.1 M) as eluting agents.

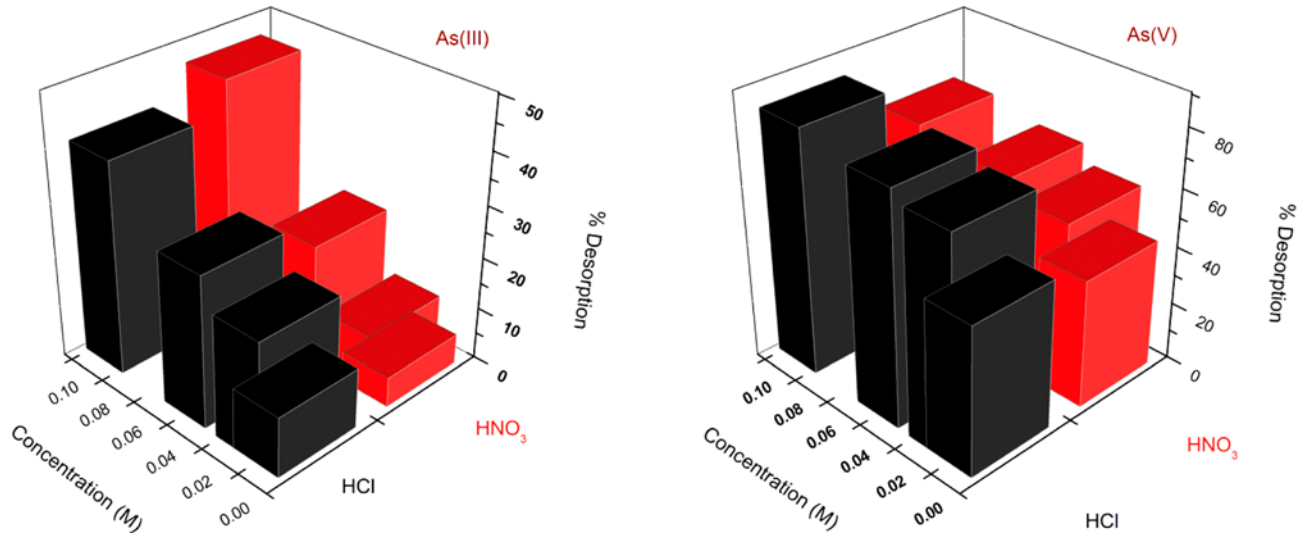

Fig. 10. Comparative desorption of As(III) and As(V) from exhausted biomass of PGP.

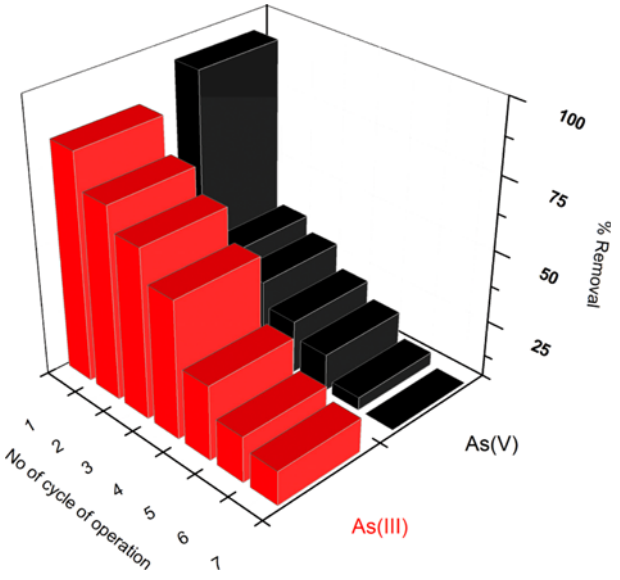

Fig. 11. Percent removal of As(III) and As(V) by PGP at up 7th cycles of batch operation.

Effective reuse of the adsorbent is directly linked to cost: only such biosorbents that can be reused and have practical importance in real life. The reusability of PGP was tested with their dried mass. The percentage arsenic removal by PGP was found to decrease (Fig. 11) from 96% to 10% in the case of As(V), while that in case As(III) 86% to 18% follows the sequence of first to seventh cycles of operation.

CONCLUSIONS

On the basis of results of characterization and adsorption studies of As(III) and As(V) on PGP, the following conclusions may be drawn:

- Batch mode of experiment reveals that the maximum percentage removal 96 for As(III) and 85.5 for As(V) was achieved at optimized conditions of temperature, biosorbent dose, arsenic concentration, contact time and pH, indicating that biosorbent can be used directly without any chemical treatments.
- The presence of common cations such as Fe^{3+}, Zn^{2+}, K^{+} enhances the adsorption efficiency whereas Cr^{6+}, Pb^{2+}, Cu^{2+}, Ni^{2+} and Ca^{2+} reduces the adsorption capacity. On the other hand, anions like NO_3^-, Cl^-, do not significantly influence the adsorption efficiency, whereas F^- and SO_4^{2-} reduces the percent removal efficiency of PGP.
- The adsorption mean energy (E) was found to be 0.259 and 0.447 $kJmol^{-1}$ for As(III) and As(V), respectively, suggesting the kind of adsorption as physical.
- The regeneration properties of biosorbent (PGP) prove its economic importance for arsenic removal from water.
- The negative values of ΔG^o of entire temperature range stipulate the spontaneity of adsorption process. Further, the positive magnitude of As(III) and As(V) confirms the nature of the process as endothermic. The sticking probability (S^*) 0.0095 for As(III) and 0.0126 for As(V) also indicates the physical nature of the process.
- The examination of all six error functions shows that the Langmuir isotherm for As(III) and Temkin isotherm for As(V) provide best-fit towards experimental equilibrium data.

ACKNOWLEDGEMENT

The authors would like to extend their sincere thanks to the Birla Institute of Technology for financial support and we are also thankful to Central Instrumentation Facility (CIF), BIT, Mesra, for useful assistance in sample analysis.

REFERENCES

1. P. K. Pandey, S. Yadav, S. Nair and A. Bhui, *Environ. Int.*, **28**, 235 (2002).
2. S. Bhattacharjee, S. Chakravarty, S. Maity, V. Dureja and K. Gupta,

Chemosphere, **58**, 1203 (2005).
3. E. Roy, S. Patra, R. Madhuri and P. K. Sharma, *Chem. Eng. J.*, **304**, 259 (2016).
4. P. Smedley and D. Kinniburgh, *Appl. Geochem.*, **17**, 517 (2002).
5. A. Basu, D. Saha, R. Saha, T. Ghosh and B. Saha, *Res. Chem. Intermed.*, **40**, 447 (2014).
6. D. Mohan and C. U. Pittman, *J. Hazard. Mater.*, **142**, 1 (2007).
7. M. Abid, N. K. Niazi, I. Bibi, A. Farooqi, Y. S. Ok, A. Kunhikrishnan, F. Ali, S. Ali, A. D. Igalavithana and M. Arshad, *Int. J. Phytoremed.*, **18**, 442 (2016).
8. C. Jain and I. Ali, *Water Res.*, **34**, 4304 (2000).
9. A. N. S. Saqib, A. Waseem, A. F. Khan, Q. Mahmood, A. Khan, A. Habib and A. R. Khan, *Ecol. Eng.*, **51**, 88 (2013).
10. B. K. Mandal and K. T. Suzuki, *Talanta*, **58**, 201 (2002).
11. M. B. Shakoor, N. K. Niazi, I. Bibi, G. Murtaza, A. Kunhikrishnan, B. Seshadri, M. Shahid, S. Ali, N. S. Bolan and Y. S. Ok, *Critical Rev. Environ. Sci. Technol.*, **46**, 467 (2016).
12. J. F. Ferguson and J. Gavis, *Water Res.*, **6**, 1259 (1972).
13. P. Roy and A. Saha, *Current Sci.*, **82**, 38 (2002).
14. K. Baidya, A. Raj, L. Mondal, G. Bhaduri and A. Todani, *J. Ocular Pharmacol. Therap.*, **22**, 208 (2006).
15. P. Ghosh, M. Banerjee, S. De Chaudhuri, R. Chowdhury, J. K. Das, A. Mukherjee, A. K. Sarkar, L. Mondal, K. Baidya and T. J. Sau, *J. Exp. Sci. Environ. Epidemiol.*, **17**, 215 (2007).
16. S. C. Mukherjee, M. M. Rahman, U. K. Chowdhury, M. K. Sengupta, D. Lodh, C. R. Chanda, K. C. Saha and D. Chakraborti, *J. Environ. Sci. Health, Part A*, **38**, 165 (2003).
17. C. H. Tseng, *Toxicol. Appl. Pharmacol.*, **197**, 67 (2004).
18. S. Wickramasinghe, B. Han, J. Zimbron, Z. Shen and M. Karim, *Desalin.*, **169**, 231 (2004).
19. M. B. Baskan and A. Pala, *Desalin.*, **281**, 396 (2011).
20. T. Viraraghavan, K. Subramanian and J. Aruldoss, *Water Sci. Technol.*, **40**, 69 (1999).
21. M. Gholami, M. Mokhtari, A. Aameri and M. A. Fard, *Desalin.*, **200**, 725 (2006).
22. I. W. Ouédraogo, E. Pehlivan, H. T. Tran, S. Paré, Y. L. Bonzi-Coulibaly, D. Zachmann and M. Bahadir, *Toxicol. Environ. Chem.*, **98**, 736 (2016).
23. A. Ashraf, I. Bibi, N. K. Niazi, Y. S. Ok, G. Murtaza, M. Shahid, A. Kunhikrishnan, D. Li and T. Mahmood, *Int. J. Phytorem.*, **19**, 605 (2017).
24. J. A. Baig, T. G. Kazi, A. Q. Shah, G. A. Kandhro, H. I. Afridi, S. Khan and N. F. Kolachi, *J. Hazard. Mater.*, **178**, 941 (2010).
25. U. Shafique, A. Ijaz, M. Salman, W. uz Zaman, N. Jamil, R. Rehman and A. Javaid, *J. Taiwan Ins. Chem. Eng.*, **43**, 256 (2012).
26. D. Ranjan, M. Talat and S. Hasan, *J. Hazard. Mater.*, **166**, 1050 (2009).
27. A. Bhatnagar, V. J. Vilar, C. M. Botelho and R. A. Boaventura, *Adv. Colloid Interface Sci.*, **160**, 1 (2010).
28. W. S. Choi and J. H. Han, *J. Food Sci.*, **66**, 319 (2001).
29. Q. Wen, Y. Wu, L.-x. Zhao, Q. Sun and F.-y. Kong, *J. Zhejiang Univer. Sci. B*, **11**, 87 (2010).
30. Y.-G. Yan and J.-H. Tay, *Water Res.*, **31**, 1573 (1997).
31. X. Liu, H. Ao, X. Xiong, J. Xiao and J. Liu, *Water, Air, Soil Pollut.*, **223**, 1033 (2012).
32. A. Gupta and N. Sankararamakrishnan, *Bioresour. Technol.*, **101**, 2173 (2010).
33. K. Anoop Krishnan, K. Sreejalekshmi and R. Baiju, *Bioresour. Technol.*, **102**, 10239 (2011).
34. I. Ali and V. Gupta, *Nat. Protocol.*, **1**, 2661 (2006).
35. S. Lagergren, *Eur. Polym. J.*, **9**, 525 (1898).
36. P. Roy, N. K. Mondal, S. Bhattacharya, B. Das and K. Das, *Appl. Water Sci.*, **3**, 293 (2013).
37. Y.-S. Ho and G. McKay, *Process Biochem.*, **34**, 451 (1999).
38. K. Singh, M. Talat and S. Hasan, *Bioresour. Technol.*, **97**, 2124 (2006).
39. S. Kuppusamy, P. Thavamani, M. Megharaj, K. Venkateswarlu, Y. B. Lee and R. Naidu, *Proc. Safety Environ. Protection*, **100**, 173 (2016).
40. R. Jha, U. Jha, R. Dey, S. Mishra and S. Swain, *Desalin. Water Treat.*, **53**, 2144 (2015).
41. V. K. Gupta, A. Nayak and S. Agarwal, *Environ. Eng. Res.*, **20**, 1 (2015).
42. M. Leist, R. Casey and D. Caridi, *J. Hazard. Mater.*, **76**, 125 (2000).
43. S. Kundu and A. Gupta, *Chem. Eng. J.*, **122**, 93 (2006).
44. K. Singh, R. Rastogi and S. Hasan, *J. Hazard. Mater.*, **121**, 51 (2005).
45. H. Rezaei, *Arabian J. Chem.*, **9**, 846 (2016).
46. P. K. Pandey, S. Choubey, Y. Verma, M. Pandey and K. Chandrashekhar, *Bioresour. Technol.*, **100**, 634 (2009).
47. R. Karthik and S. Meenakshi, *J. Water Proc. Eng.*, **1**, 37 (2014).
48. M. H. Dehghani, A. Zarei, A. Mesdaghinia, R. Nabizadeh, M. Alimohammadi and M. Afsharnia, *Korean J. Chem. Eng.*, **34**, 757 (2015).
49. C. Namasivayam and M. Sureshkumar, *Bioresour. Technol.*, **99**, 2218 (2008).
50. S. K. Maji, A. Pal and T. Pal, *J. Hazard. Mater.*, **151**, 811 (2008).
51. D. Mohan and C. U. Pittman, *J. Hazard. Mater.*, **137**, 762 (2006).
52. M. C. Ncibi, *J. Hazard. Mater.*, **153**, 207 (2008).
53. Y. S. Ho, *Water Res.*, **37**, 2323 (2003).
54. J. Igwe and A. Abia, *Glob. J. Environ. Res.*, **1**, 22 (2007).

REFERENCES (Table 7)

1. P. Okafor, P. Okon, E. Daniel and E. Ebenso, *Int. J. Electrochem. Sci.*, **7**, 12354 (2012).
2. U. Shafique, A. Ijaz, M. Salman, W. uz Zaman, N. Jamil, R. Rehman and A. Javaid, *J. Taiwan Inst. Chem. Eng.*, **43**, 256 (2012).
3. S. Kamsonlian, S. Suresh, V. Ramanaiah, C. Majumder, S. Chand and A. Kumar, *Intern. J. Environ. Sci. Technol.*, **9**, 565 (2012).
4. V. M. Marín-Rangel, R. Cortés-Martínez, R. A. Cuevas Villanueva, M. Garnica-Romo and H. E. Martínez-Flores, *J. Food Sci.*, **77**, T10 (2012).
5. Y. Tian, M. Wu, X. Lin, P. Huang and Y. Huang, *J. Hazard. Mater.*, **193**, 10 (2011).
6. D. Ranjan, M. Talat and S. Hasan, *J. Hazard. Mater.*, **166**, 1050 (2009).
7. T. Anirudhan and M. R. Unnithan, *Chemosphere.*, **66**, 60 (2007).
8. K. N. Ghimire, K. Inoue, K. Makino and T. Miyajima, *Sep. Sci. Technol.*, **37**, 2785 (2002).
9. X. Liu, H. Ao, X. Xiong, J. Xiao and J. Liu, *Water, Air, Soil Pollut.*, **223**, 1033 (2012).
10. E. Pehlivan, H. Tran, W. Ouédraogo, C. Schmidt, D. Zachmann and M. Bahadir, *Food Chem.*, **138**, 133 (2013).
11. S. Bibi, A. Farooqi, A. Yasmeen, M. A. Kamran and N. K. Niazi, *Intern. J. Phytorem.* (2017).